Comparative Analyses of *N*-Glycosylation Profiles of Influenza A Viruses Grown in Different Host Cells

Hirokazu Yagi[1], Shinya Watanabe[2], Takashi Suzuki[2], Tadanobu Takahashi[2], Yasuo Suzuki[3], and Koichi Kato*[,1, 4, 5, 6]

[1]*Graduate School of Pharmaceutical Sciences, Nagoya City University, 3-1 Tanabe-dori, Mizuho-ku, Nagoya 467-8603, Japan*

[2]*Department of Biochemistry, University of Shizuoka, School of Pharmaceutical Sciences, and Global COE Program for Innovation in Human Health Sciences, Yada, Shizuoka 422-8526, Japan*

[3]*Department of Biomedical Sciences College of Life and Health Sciences, Chubu University, 1200 Matsumoto-cho, Kasugai 487-8501, Japan*

[4]*Institute for Molecular Science and Okazaki Institute for Integrative Bioscience, National Institutes of Natural Sciences, 5-1 Higashiyama Myodaiji, Okazaki 444-8787, Japan*

[5]*GLYENCE Co., Ltd., 2-22-8 Chikusa, Chikusa-ku, Nagoya 464-0858, Japan*

[6]*The Glycoscience Institute, Ochanomizu University, 2-1-1 Ohtsuka, Bunkyo-ku, Tokyo 112-8610, Japan*

Abstract: Glycosylation of the surface glycoproteins of influenza A virus is associated with several viral properties such as receptor binding and susceptibility to neuraminidase inhibitors. In this study, we evaluated the detailed structures of *N*-glycans derived from the same influenza virus strain A/Memphis/1/71 (H3N2) grown in different host cells, i.e., Madin-Darby canine kidney (MDCK) cells and embryonated eggs. Although both influenza virus isolates expressed neutral and sulfated oligosaccharides, their detailed profiles were significantly different. In contrast, *N*-glycosylation profiles of the influenza virus isolate from MDCK cells were highly homologous with those of desialylated *N*-glycans derived from its host cells. These data demonstrate that the glycosylation of influenza viruses is governed by their host cells.

Keywords: Influenza virus A / *N*-glycans / HPLC mapping / host specific glycosylation.

INTRODUCTION

Influenza is one of the most widely-distributed zoonotic infectious diseases in the world, and its pathogen, the influenza virus, can be isolated from various animals including humans [1,2]. The envelopes of the influenza viruses have two spike glycoproteins: hemagglutinin (HA) and neuraminidase (NA). The HA spike glycoprotein is responsible for the binding of the virus to host cell receptors, sialo-sugar chains of glycoproteins and glycolipids, and also for the removal of the viral envelope by fusion between the cellular endosomal/lysosomal and viral membranes [1]. The NA spike glycoprotein exhibits sialidase activity that cleaves sialic acid from viral receptor sialo-sugar chains. This process is essential for virus budding from the host cell membranes. Despite *N*-glycosylation of both HA and NA, the mature, active influenza virion's envelope does not possess sialic acid [3].

*Address correspondence to this author at the Graduate School of Pharmaceutical Sciences, Nagoya City University, 3-1 Tanabe-dori, Mizuho-ku, Nagoya 467-8603, Japan; Tel: +81-52-836-3447; Fax: +81-52-836-3447;
E-mail: kkato@phar.nagoya-cu.ac.jp

The *N*-linked oligosaccharides of enveloped viruses play a role in viral activities, such as receptor binding [4-6], membrane fusion [7], viral replication and growth [8,9], and translational folding and transport process of viral proteins [10,11] . Structural studies indicated that the HA derived from A/WSN/33 (H1N1) and A/Hong Kong/1/68 (H3N2) strains grown in Madin-Darby Bovine Kidney (MDBK) cells exhibited different *N*-glycosylation profiles [12,13]. In addition, *N*-glycans of H3N2 viruses grown in different host cells have been demonstrated to have distinct susceptibilities to endoglycosidases H and F [14]. These findings indicate that the *N*-glycosylation profiles of influenza viruses depend on their host. However, no study has yet been reported to compare *N*-glycosylation profiles of the same viral strains grown in different host cells. In view of this situation, we herein describe the detailed structures of *N*-glycans derived from distinct virus isolates grown in embryonated eggs and Madin-Darby canine kidney (MDCK) cells. The embryonated egg has been one of the most widely used vehicles for production of influenza virus vaccines. On the other hand, MDCK cells have been utilized for culturing and isolation of influenza viruses and their infection experiments in laboratories, because viral mutation seldom occurs during passage in the cells. *N*-glycosylation profiles of these virus isolates are provided with linkage information based on multi-

1875-3981/12

dimensional HPLC mapping in conjunction with mass spectrometric (MS) data.

MATERIALS AND METHODOLOGY

Materials

Materials used for the experiments were purchased from the sources indicated below: Glycoamidase A from sweet almond, β-galactosidase and β-*N*-acetylhexosaminidase from jack bean were purchased from Seikagaku Kogyo Co. (Tokyo, Japan). α-Galactosidase from green coffee bean was purchased from Oxford Glycosystems Inc. (Bedford**,** MA). α-Sialidase from *Arthrobacter ureafaciens* was purchased from Nacalai Tesque (Kyoto, Japan). α-2,3-Sialidase from *Salmonella typhimurium* was purchased from Takara Bio Inc.(Otsu, Japan). Trypsin and chymotrypsin were purchased from Sigma (St Louis, MO, USA). The PA-derivatives of isomalto-oligosaccharides (4–20 glucose residues) and those of *N*-linked oligosaccharides having code numbers M4.1, M5.1, M6.1, M7.1, M7.2, M8.1, M8.2, M9.1, H5.12, H4.12, 100.4, 200.1, 200.3, 200.4, 200.41, 200.42, 200.43, 210.2, 210.3, 210.4, 210.41, 210.41, 210.42, 210.43, 201.4, 201.41, 211.2, 211.3, 211.4, 211.41, 211.42, 211.43, 300.1, 311.1, 300.22, 300.8, 310.8, and 311.8 in the GALAXY database (http://www.glycoanalysis.info/galaxy2/ENG/index.jsp) [15,16], were purchased from Seikagaku Kogyo Co. and GLYENCE Co.(Nagoya, Japan). The PA-oligosaccharides sulfated at the C6 position of *N*-acetylglucosamine residues (code nos. 1S1-200.4, 1S2-200.4, 1S1-200.41, 1S1-210.4, 1S2-210.4, 1S1-210.1, 1S2-210.1, 1S1-211.4, and 1S1-211.41) were prepared as described in a previous study [17].

Virus Preparation

The influenza virus strain A/Memphis/1/71 (H3N2) used in this study were propagated in 10-day-old embryonated chicken eggs or in MDCK cells the in serum free medium, Hybridoma-SFM (Invitrogen, Carlsbad, CA) containing acetylated trypsin (2.0 μg/ml) and purified as described previously [18,19].

Fetuin Binding Assay

Fetuin-binding activity of influenza A viruses grown in embryonated eggs and MDCK cells was determined by a solid-phase binding assay. Fifty microliters of fetuin (1 mg/ml; Sigma) was added to wells of microtiter plates (F96 Maxisorp; Nalge Nunc, Wiesbaden, Germany) and incubated at 4°C for 5 h. After the plates were washed five times with phosphate-buffered saline (PBS), the remaining binding site on the wells was blocked with 250 μl of PBS containing 0.01% Tween 20 (T-PBS) at 4°C for 12 h. After the plates were washed five times with T-PBS, 50μl of each influenza A virus suspension [1-1024 HAU (hemagglutination units)] in T-PBS was added to the wells and incubated on ice for 3 h. As a control, fetuin-coated wells were incubated without viruses. Unbound viruses were removed by washing with T-PBS. Fifty microliters of rabbit anti-A/Memphis/1/71 (H3N2) antibody diluted 1:200 with T-PBS was added to the wells. After incubation on ice for 2 h, the plates were washed five times with T-PBS and again incubated on ice for 2 h with 50μl of horseradish peroxidase-conjugated protein A (Sigma) diluted 1:200 with T-PBS. After the plates were washed five times with T-PBS, the amount of bound virions was determined by measuring the absorbance at 492 nm with *O*-phenylenediamine reagent as previously described [20].

HPLC Mapping Method

All experimental procedures, including the delipidation of influenza A viruses and MDCK cells, chromatographic conditions, glycosidase treatments, and the matrix-assisted laser desorption/ionization time-of-flight mass spectrometric (MALDI-TOF-MS) technique, have been described previously [17,21,22]. The delipidated extract was proteolyzed with chymotrypsin and trypsin mixture and digested with glycoamidase A to release *N*-glycans. After peptide removal, the reducing ends of the *N*-glycans were derivatized with 2-aminopyridine. The mixture of PA-derivatives of the *N*-glycans was separated by HPLC on a TSK gel DEAE-5PW column (Tosoh, Tokyo, Japan). The fractionated PA-glycans were then individually separated and identified sequentially on a Shim-pack HRC-ODS column (Shimadzu, Kyoto, Japan) and on a TSK-gel Amide-80 column (Tosoh, Tokyo, Japan). The identification of *N*-glycan structures was based on their elution positions on these three types of columns compared with PA-glycans in the GALAXY database [15,16]. The structures of the PA-glycans that are not registered in the GALAXY database were characterized by HPLC mapping in conjunction with exoglycosidase treatments, desulfation, and MALDI-TOF-MS analysis with an AXIMA-CFR MALDI-TOF MS spectrometer (Shimadzu).

Parts of the PA-glycans derived from the MDCK cells were treated with α-sialidase before HPLC analysis.

RESULTS AND DISSCUSSION

Recently, it has been reported that the glycosylation of influenza HA affects receptor binding and immune response [23,24]. In this study, we compared fetuin-binding activities between the influenza A virus isolates grown in MDCK cells and embryonated eggs. As shown in Fig. (**1**), the MDCK-derived viruses exhibited a higher affinity for fetuin than those originating from embryonated eggs. Since both virus isolates shared identical amino acid sequences of the spike glycoproteins, it is most likely that the observed difference in fetuin-binding activity is attributed to their distinct glycosylation profiles. Hence, we conducted *N*-glycosylation profiling of these virus preparations along with the host MDCK cells.

N-glycans were liberated from the protein extracts of influenza A viruses grown in different host cells (embryonated eggs and MDCK cells) and MDCK cells by glycoamidase A, labeled with 2-aminopyridine, and then subjected to DEAE column chromatography. Influenza virus isolates from the different host cells showed both neutral and anionic oligosaccharides (Fig. **2A** and **2B**). As shown in Fig. (**2C**), the *N*-glycans derived from both virus isolates comprised approximately 90% neutral and 10% anionic oligosaccharides. MALDI-TOF-MS data indicated that all anionic oligosaccharides were sulfated but not sialylated. These data are consistent with previous reports [3]. To compare the *N*-glycans expressed in the virus with that in its hosts, we analyzed *N*-glycosylation of MDCK cells. In the DEAE profile

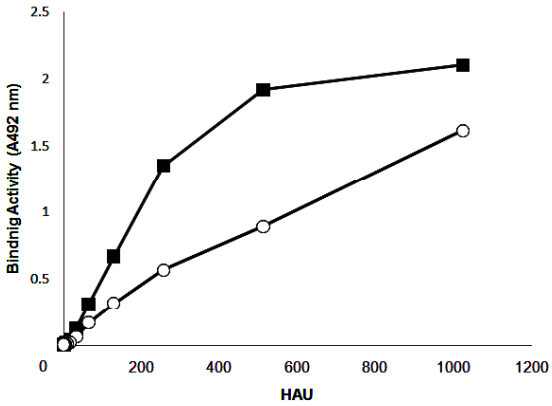

Fig. (1). Binding of influenza A virus isolates to fetuin.

The binding of influenza viruses grown in embryonated eggs (open circle) and MDCK cells (filled square) were measured by a solid-phase binding assay. The amount of bound virions was determined by measuring the absorbance at 492 nm with *O*-phenylenediamine reagent.

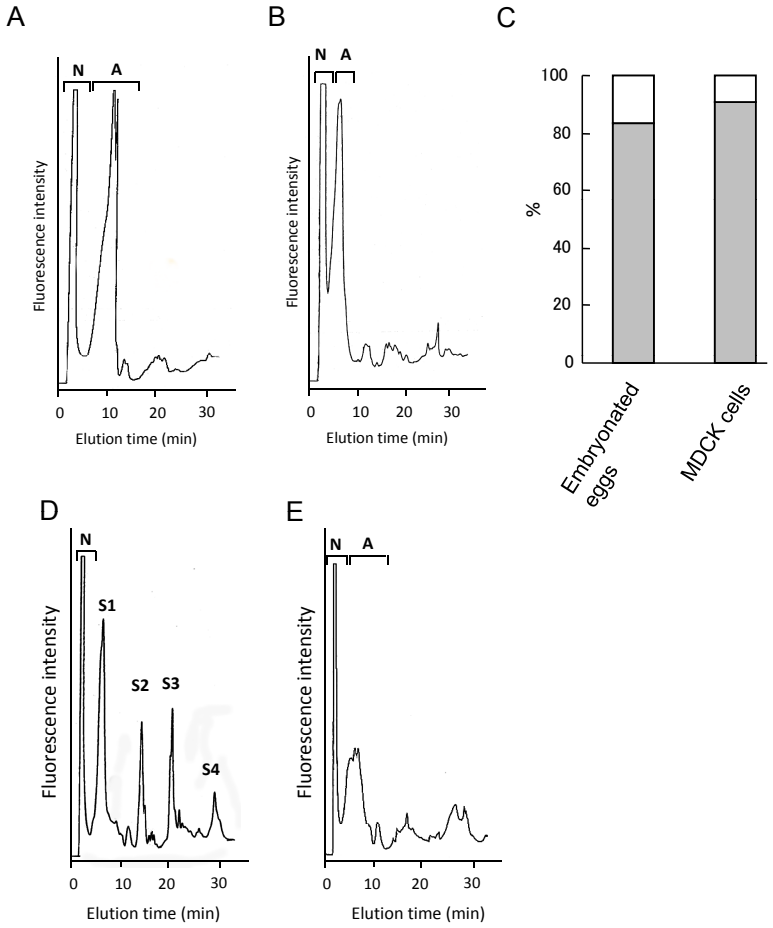

Fig. (2). HPLC profiles of PA-glycans, derived from influenza viruses and the host cells, on the DEAE column. Chromatograms of PA-oligosaccharides derived from influenza A viruses grown in embryonated eggs (**A**) and in MDCK cells (**B**), and host MDCK cells (**D** and **E**). (**C**) The ratio of neutral and anionic oligosaccharides was calculated from the peak intensity. MALDI-TOF-MS data indicated that all anionic glycans in the influenza viruses were sulfated. The *N*-glycans derived from MDCK cells were applied to a DEAE column before (**D**) and after (**E**) α-sialidase treatment. S1, S2, S3, and S4 indicate the fractions that contain mono-, di-, tri-, and tetra-sialyl oligosaccharides.

derived from the delipidated MDCK cell extract, several anionic fractions were detected because of sialylation (Fig. **2D**). To compare sulfation in the two virus preparations, the PA-glycan mixture was subjected to α-sialidase treatment. The desialylated product was applied to the DEAE column to fractionate neutral and sulfated oligosaccharides (Fig. **2E**).

The neutral and sulfated oligosaccharide fractions derived from the two different virus preparations and the MDCK cells were applied individually to the ODS column (Fig. **3A-F**). Subsequently, the individual fractions separated from the ODS column were applied to an amide column. We isolated neutral and anionic oligosaccharides and recorded

the elution times of these PA-glycans on the ODS and amide columns. The PA-oligosaccharides were identified on the basis of correspondence of their elution data with those in the GALAXY database. For example, the major *N*-glycan corresponding to peak 1 was eluted at 4.9 glucose unit (GU) on the ODS column and at 8.9 GU on the amide column. The elution data set was in good agreement with those of a known reference *N*-glycan, Man-α-(1→2)Man-α-(1→6)-[Man-α-(1→3)-]Man-α-(1→6)-[Man-α-(1→2)Man-α-(1→2)-Man-α-(1→3) -]Man-β-(1→4)-GlcNAc-β-(1→4)-GlcNAc-PA (code no. M8.1 in the GALAXY database). By co-chromatography using the standard PA-glycans and MALDI-TOF-MS analysis, the structure of this PA-oligosaccharide was confirmed. PA-glycans corresponding to the peaks N-16-1, N-24-2, N-28-1, N-29-2, and all sulfated fractions, except A-e-2, A-g-1, A-m-1, and A-n-1, were not registered in the GALAXY database. Accordingly, these PA-glycans were trimmed by exoglycosidase and HCl treatments to become identical to known glycans [17,21,22]. Considering the specificities of the exoglycosidases used and the MALDI-TOF-MS data, the original structures of these PA-glycans were unambiguously determined except for the sulfated position on the non-reducing terminal β-galactose residues (Table **2**). Sulfation at the C3 position of galactose and C6 position of *N*-acetylglucosamine residues has been reported in the influenza virus isolates from MDCK cells and its host [25]. This report strongly suggests that sulfation also occurred at the C3 position of the non-reducing terminal galactose residues in the specimens used in the present study.

Tables **1** and **2** summarize the structures and incidences (mol%) of the identified *N*-glycans. HPLC mapping revealed the detailed structures of *N*-glycans on influenza virus grown in embryonated eggs and MDCK cells, which exhibited distinct *N*-glycosylation patterns. For example, the high-mannose-type glycan corresponding to peak N-2-2 was much more prevalent in viruses grown in the MDCK cells (10.2%) than in those grown in the embryonated eggs (2.3%). The Lewis X-containing oligosaccharides (e.g.,N-12-1) were detected only in the egg-derived viruses, while the galabiose structures (e.g., N-16-1) were identified only in the virus isolate from MDCK cells. In addition, the profiles of the sulfated oligosaccharides different between the two virus isolates (Table **3**).

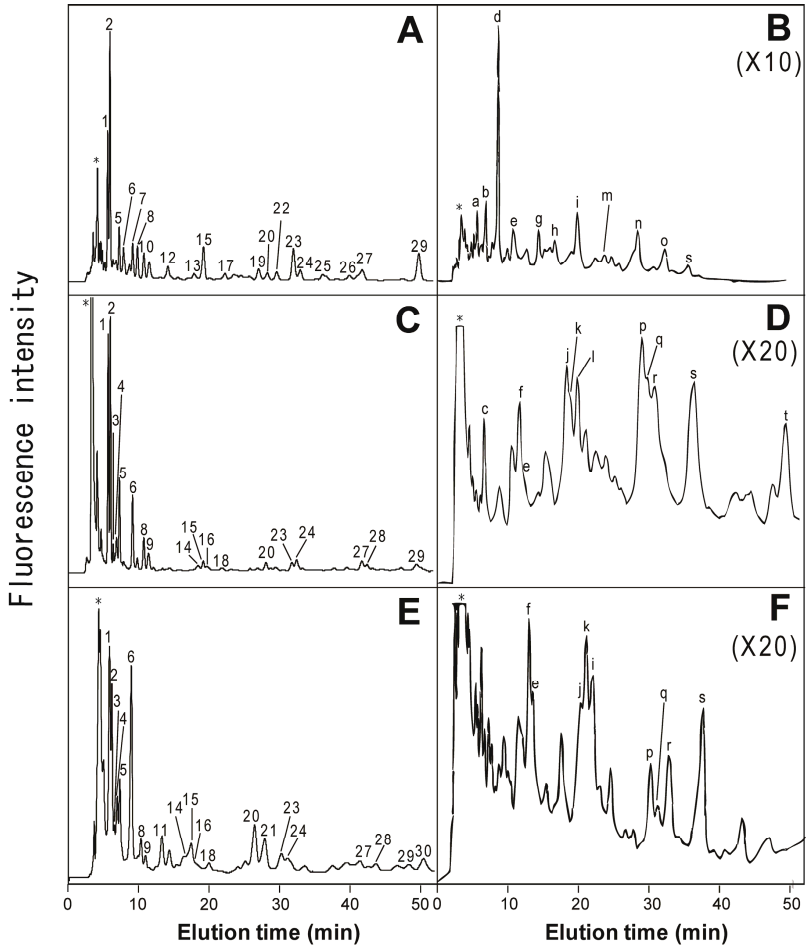

Fig. (3). HPLC profiles on the ODS column of PA-glycans derived from influenza viruses and the host cells. Chromatograms of PA-oligosaccharides derived from influenza A viruses grown in embryonated eggs (**A** and **B**) and MDCK cells (**C** and **D**), and the host MDCK cells treated by sidalidase (**E** and **F**). The fractions of the neutral and sulfated oligosaccharides were separated on the DEAE column in advance. A, C, and E, neutral *N*-glycans; B, D, and F, sulfated *N*-glycans. In A and C, the peaks were numbered in order of GU (ODS), with missing numbers 11, 21, and 30, which correspond to the fractions detected only in the protein extracts from the MDCK cells (in E). In B, D, and F, peaks were recorded alphabetically in order of elution. Asterisks indicate the fractions containing no detectable PA-oligosaccharides. B was adapted from the literature [16].

Table 1. HPLC Data and Relative Quantities of the Neutral N-glycans Derived from Two Different Virus Preparations and the Desialylated, Non-sulfated PA-oligosacchraides Derived from MDCK Cells

Peaks	GU(ODS)	PA-Oligosaccharides	Relative Quantity (%)[a]		
	GU(amide)		Virus (egg)	Virus (MDCK)	Host (MDCK)
N-1-1	4.9 8.9	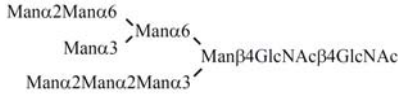	8.7	18.3	11.6
N-2-1	5.1 8.0	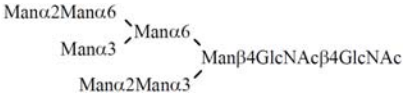	13.3	10.6	4.2
N-2-2	5.1 9.7	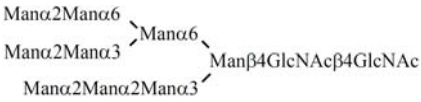	1.9	8.4	3.4
N-3-1	5.4 8.5	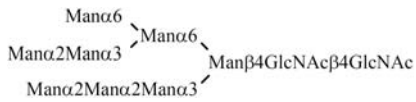	—	8.4	3.4
N-4-1	5.9 7.9	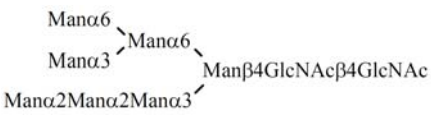	—	2.4	3.5
N-5-1	6.1 7.0	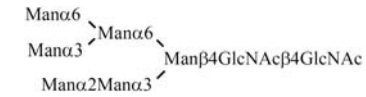	3.2	6.9	4.6
N-6-1	7.1 6.1	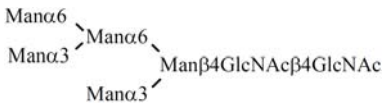	3.3	8	14.4
N-7-1	7.5 5.1	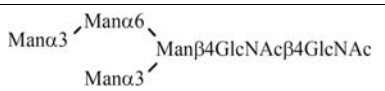	3.1	—	—
N-8-1	7.9 7.4	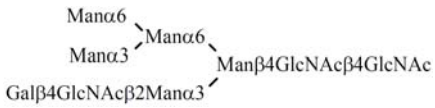	2.8	3.9	1.4
N-9-1	8.1 6.4	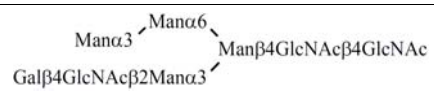	—	2.3	0.7
N-10-1	8.1 5.7	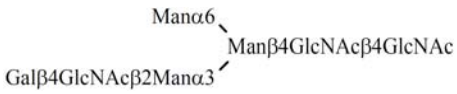	2.3	—	—
N-11-1	8.9 5.1	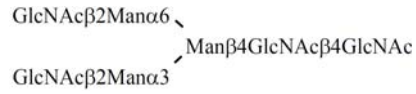	—	—	3.3
N-12-1	9.1 7.4	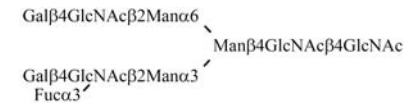	2.2	—	—
N-13-1	10.1 7.4	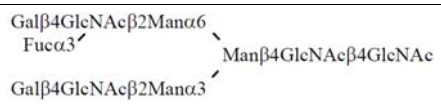	0.8	—	—

Table 1. Contd…..

Peaks	GU(ODS) / GU(amide)	PA-Oligosaccharides	Relative Quantity (%)[a] Virus (egg)	Virus (MDCK)	Host (MDCK)
N-14-1	10.3 8.1	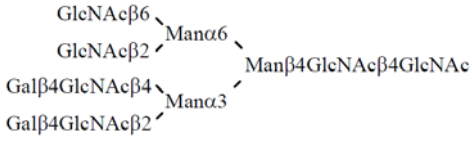	—	1.1	—
N-15-1	10.5 7.0	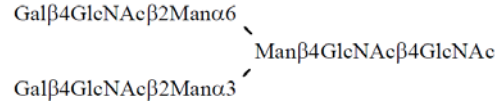	5.3	1.6	5.2
N-16-1	10.7 7.5	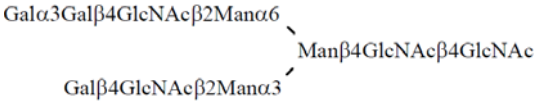	—	1.0	1.0
N-17-1	11.3 9.0	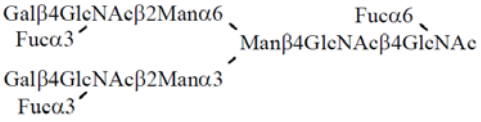	1.0	—	—
N-18-1	11.0 5.5	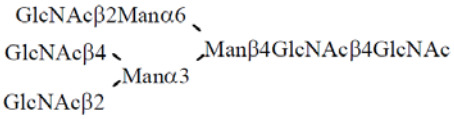	—	0.8	0.8
N-19-1	12.8 8.1	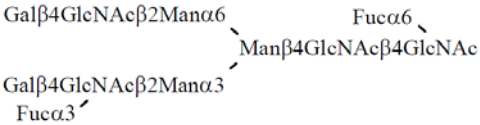	1.9	—	—
N-20-1	13.2 8.3	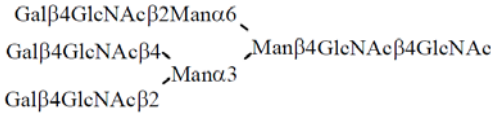	1.1	1.4	7.7
N-21-1	13.3 8.2	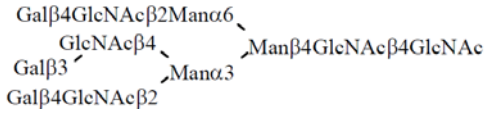	—	—	5.6
N-22-1	13.7 7.3	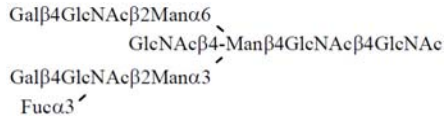	1.5	—	—
N-23-1	14.4 7.4	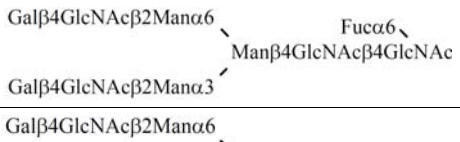	6.1	2.1	2.8
N-24-1	14.9 7.2	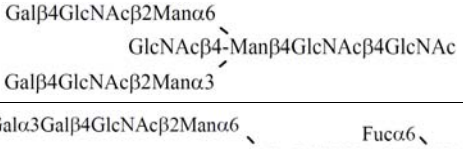	1.9	—	1.3
N-24-2	14.9 8.1	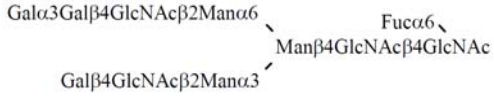	—	3.0	0.7
N-24-3	14.9 10.3	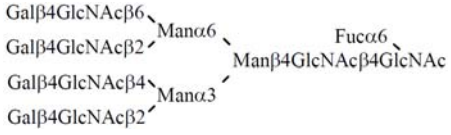	—	—	0.4

Table 1. Contd…..

Peaks	GU(ODS) / GU(amide)	PA-Oligosaccharides	Relative Quantity (%)[a] Virus (egg)	Virus (MDCK)	Host (MDCK)
N-25-1	16.1 8.7	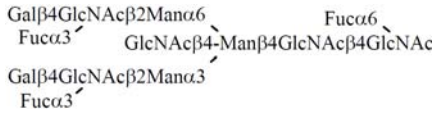	1.8	—	—
N-26-1	17.7 9.2	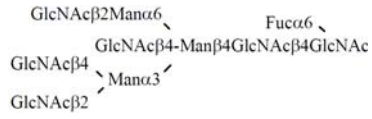	0.5	—	—
N-26-2	17.7 8.2	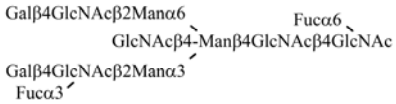	0.8	—	—
N-27-1	18.5 8.7	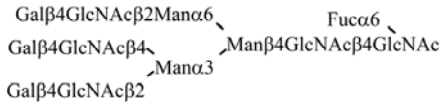	1.7	1.5	0.6
N-27-2	18.5 8.2	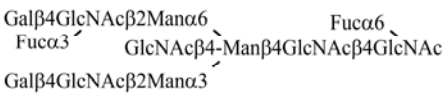	1.8	—	—
N-28-1	18.9 9.2	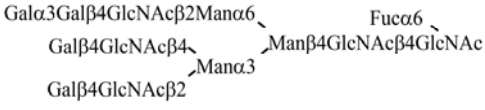	—	1.5	0.7
N-29-1	20.5 7.5	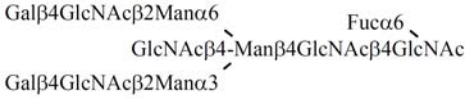	6.5	1.6	1.8
N-29-2	20.5 8.1	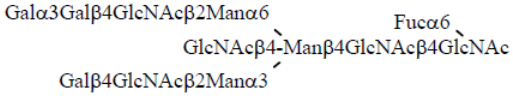	—	0.7	0.4
N-30-1	22.1 9.2	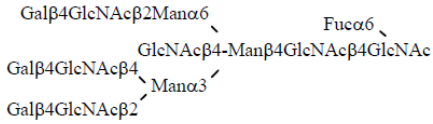	—	—	1.5
Others			9.9	5.5	7.1

a) Relative quantities were calculated from peak areas of total neutral oligosaccharides in each chromatogram on the ODS column.

Table 2. HPLC Data and Relative Quantities of the Sulfated *N*-glycans Derived from Two Different Virus Preparations, and Desialylated, Sulfated PA-oligosacchraides Derived from MDCK Cells

Peaks	GU(ODS) / GU(amide)	PA-Oligosaccharides	Relative Quantity (%)[a] Virus (egg)	Virus (MDCK)	Host (MDCK)
A-a-1	6.2 5.2	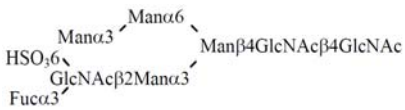	0.2	—	—
A-a-2	6.4 5.7	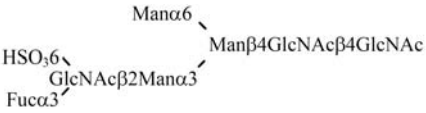	0.1	—	—

Table 2. Contd…..

Peaks	GU(ODS) / GU(amide)	PA-Oligosaccharides	Relative quantity (%)[a]		
			Virus (egg)	Virus (MDCK)	Host (MDCK)
A-b-1	8.0 6.9	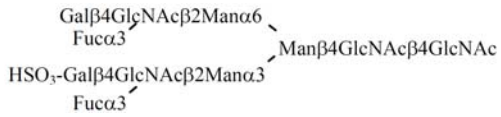	0.7	—	—
A-c-1	8.3 5.8	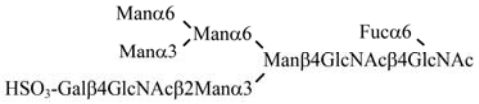	—	0.3	—
A-c-2	8.3 5.9	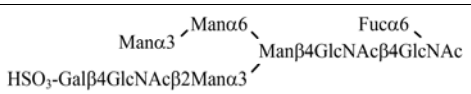	—	0.1	—
A-d-1	8.4 6.2	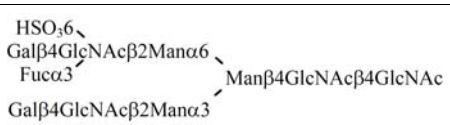	3.5	—	—
A-e-1	9.4 5.4	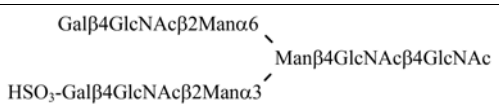	0.6	0.2	0.6
A-e-2	9.4 6.2	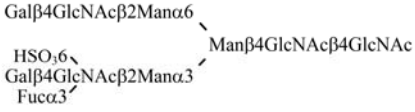	0.2	—	—
A-f-1	10.3 5.9	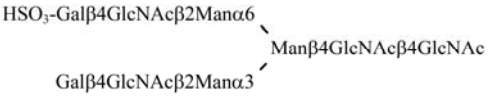	—	0.4	0.9
A-g-1	10.8 5.8	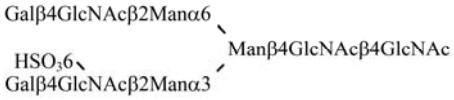	0.8	—	—
A-h-1	11.6 6.6	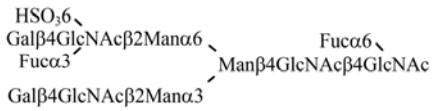	0.7	—	—
A-i-1	12.8 6.6	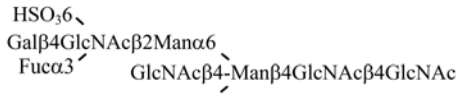	1.9	—	—
A-j-1	13.2 7.0	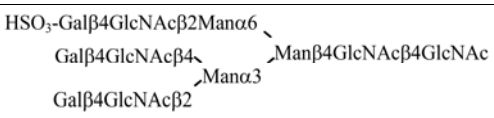	—	0.5	0.9
A-k-1	13.6 9.0	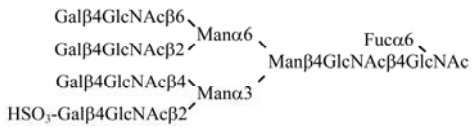	—	0.4	1.3
A-l-1	14.0 6.1	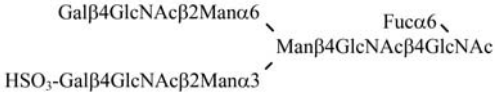	—	0.3	1.2

Table 2. Contd…..

Peaks	GU(ODS) / GU(amide)	PA-Oligosaccharides	Relative quantity (%)[a]		
			Virus (egg)	Virus (MDCK)	Host (MDCK)
A-l-2	14.0 6.8	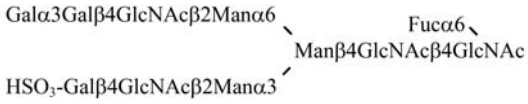	—	0.1	—
A-m-1	14.3 6.2	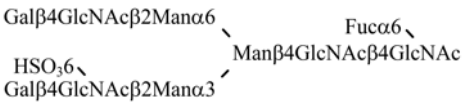	0.6	—	—
A-n-1	16.2 7.7	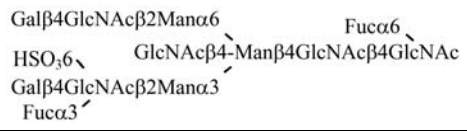	1.3	—	—
A-o-1	17.8 7.7	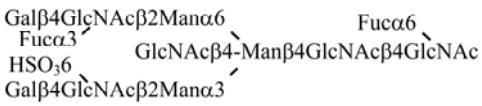	0.9	—	—
A-p-1	17.9 7.3	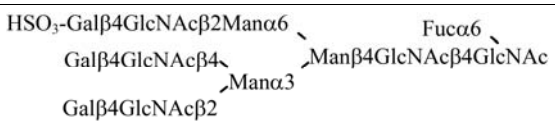	—	0.8	0.7
A-p-1	18.4 7.5	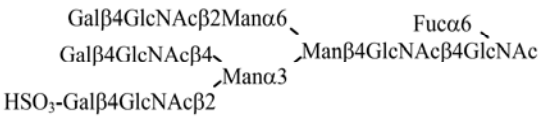	—	0.3	—
A-q-2	18.4 8.2	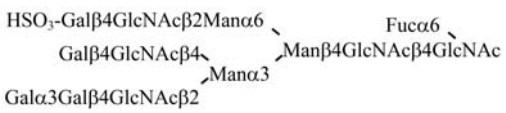	—	0.2	0.3
A-q-3	18.4 9.0	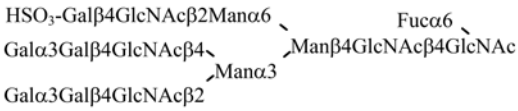	—	0.2	—
A-r-1	19.1 8.1	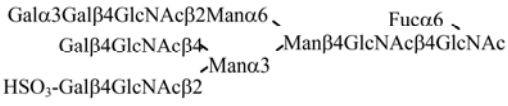	—	0.3	0.7
A-r-2	19.1 8.9	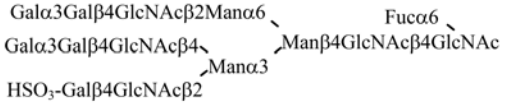	—	0.3	—
A-s-1	21.2 6.2	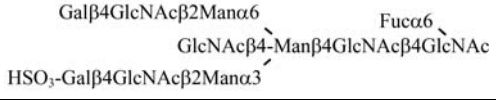	0.3	0.8	1.2
A-t-1	23.0 7.9	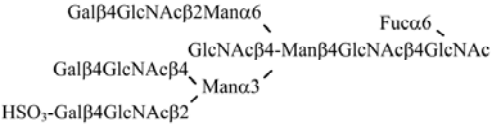	—	0.3	—
A-t-2	23.0 8.8	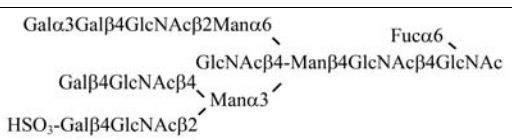	—	0.1	—
Others			4.8	3.4	4.0

a) Relative quantities were calculated from peak areas of total sulfated oligosaccharides in each chromatogram on the ODS column.

Table 3. Incidence of *N*-glycans with Specific Non-reducing Terminal Structure

Non-reducing Terminal Structures	Molar Ratio to Total *N*-glycans (%)		
	Virus (egg)	Virus (MDCK)	Host (MDCK)
Galabiose	—[a]	7.4	3.8
Sulfated *N*-acetylglucosamine	10.2	—	—
Sulfated galactose	1.6	5.6	7.8

a) Below the detection limit.

As shown in Tables 1 and 2, the MDCK cells and the virus grown in this host share considerably common *N*-glycans, characterized by the galabiose structures (e.g., N-16-1), which are not exhibited by the virus from embryonated eggs (Table **3**). Because influenza viruses do not have genes that are responsible for the biosynthesis of the sugar chains of glycoproteins and glycolipids, glycosylation of their envelopes is apparently determined by the enzymes encoded by the host genes, with the exception of NA. Here we demonstrated that the *N*-glycosylation profiles of influenza viruses are highly homologous with those of desialylated *N*-glycans derived from their host cells.

Our data strongly indicates that hosts govern the *N*-glycosylation of influenza viruses, giving rise to host-specific glycans possessing Lewis X, galabiose, and sulfated groups. This may affect the bind affinities as well as specificities of influenza viruses to the sialo-receptors and the immune responses elicited by their infection.

ACKNOWLEDGMENTS

This work was supported, in part, by Grants-in-Aid for Young Scientists (B) (H.Y., 22790076) from the Ministry of Education, Culture, Sports, Science and Technology of Japan, and by the CREST project from the Japan Science and Technology Agency. H. Y. was a recipient of a Japan Society for the Promotion of Science Research Fellowship for Young Scientists.

CONFLICT OF INTEREST

None.

REFERENCES

[1] Suzuki Y. Sialobiology of influenza: molecular mechanism of host range variation of influenza viruses. Biol Pharm Bull 2005; 28: 399-408.

[2] Suzuki Y. Comprehensive Glycoscience. Elsevier; USA 2007; pp. 465-71.

[3] Huang RT. Sphingolipids of influenza viruses. Biochim Biophys Acta 1976; 424: 90-7.

[4] Mori K, Sugimoto C, Ohgimoto S, *et al*. Influence of glycosylation on the efficacy of an Env-based vaccine against simian immunodeficiency virus SIVmac239 in a macaque AIDS model. J Virol 2005; 79: 10386-96.

[5] Ohuchi M, Ohuchi R, Feldmann A, Klenk HD. Regulation of receptor binding affinity of influenza virus hemagglutinin by its carbohydrate moiety. J Virol 1997; 71: 8377-84.

[6] Nakayama EE, Shioda T, Tatsumi M, *et al*. Importance of the N-glycan in the V3 loop of HIV-1 envelope protein for CXCR-4- but not CCR-5-dependent fusion. FEBS Lett 1998; 426: 367-72.

[7] Ohuchi R, Ohuchi M, Garten W, Klenk HD. Oligosaccharides in the stem region maintain the influenza virus hemagglutinin in the metastable form required for fusion activity. J Virol 1997; 71: 3719-25.

[8] Wagner R, Heuer D, Wolff T, *et al*. N-Glycans attached to the stem domain of haemagglutinin efficiently regulate influenza A virus replication. J Gen Virol 2002; 83: 601-9.

[9] Baigent SJ, McCauley JW. Glycosylation of haemagglutinin and stalk-length of neuraminidase combine to regulate the growth of avian influenza viruses in tissue culture. Virus Res 2001; 79: 177-85.

[10] Daniels R, Kurowski B, Johnson AE, Hebert DN. N-linked glycans direct the cotranslational folding pathway of influenza hemagglutinin. Mol Cell 2003; 11: 79-90.

[11] Ng DT, Hiebert SW, Lamb RA. Different roles of individual N-linked oligosaccharide chains in folding, assembly, and transport of the simian virus 5 hemagglutinin-neuraminidase. Mol Cell Biol 1990; 10: 1989-2001.

[12] Matsumoto A, Yoshima H, Kobata A. Carbohydrates of influenza virus hemagglutinin: structures of the whole neutral sugar chains. Biochemistry 1983; 22: 188-96.

[13] Mir-Shekari SY, Ashford DA, Harvey DJ, *et al*. The glycosylation of the influenza A virus hemagglutinin by mammalian cells. A site-specific study. J Biol Chem 1997; 272: 4027-36.

[14] Romanova J, Katinger D, Ferko B, *et al*. Distinct host range of influenza H3N2 virus isolates in Vero and MDCK cells is determined by cell specific glycosylation pattern. Virology 2003; 307: 90-7.

[15] Takahashi N, Kato K. GALAXY(Glycoanalysis by the Three Axes of MS and Chromatography):a Web Application that Assists Structural Analyses of *N*-Glycans. Trends Glycosci Glycotech 2003; 15: 235-51.

[16] Yagi H, Kato K. Multidimensional HPLC mapping method for the structural analysis of anionic *N*-glycans. Trends Glycosci Glycotech 2009; 21: 95-104.

[17] Yagi H, Takahashi N, Yamaguchi Y, *et al*. Development of structural analysis of sulfated *N*-glycans by multi-dimensional HPLC mapping methods. Glycobiology 2005; 15: 1051-60.

[18] Suzuki Y, Matsunaga M, Matsumoto M. N-Acetylneuraminyllactosylceramide, GM3-NeuAc, a new influenza A virus receptor which mediates the adsorption-fusion process of viral infection. Binding specificity of influenza virus A/Aichi/2/68 (H3N2) to membrane-associated GM3 with different molecular species of sialic acid. J Biol Chem 1985; 260: 1362-5.

[19] Takahashi T, Kurebayashi Y, Ikeya K, *et al*. The low-pH stability discovered in neuraminidase of 1918 pandemic influenza A virus enhances virus replication. PLoS One 2010; 5: 15556.

[20] Suzuki T, Jyono M, Tsukimoto M, Hamaoka A, Suzuki Y. Labeling of influenza virus with alkylamine-modified horseradish peroxidase. Anal Biochem 1995; 228: 42-7.

[21] Takahashi N, Khoo KH, Suzuki N, *et al*. *N*-glycan structures from the major glycoproteins of pigeon egg white: predominance of terminal Galα(1-4)Gal. J Biol Chem 2001; 276: 23230-9.

[22] Nakagawa H, Kawamura Y, Kato K, *et al*. Identification of neutral and sialyl *N*-linked oligosaccharide structures from human serum glycoproteins using three kinds of high-performance liquid chromatography. Anal Biochem 1995; 226: 130-8.

[23] Vries RP, Vries E, Bosch BJ, *et al*. The influenza A virus hemagglutinin glycosylation state affects receptor-binding specificity. Virology 2010; 403: 17-25.

[24] Wang CC, Chen JR, Tseng YC, *et al*. Glycans on influenza hemagglutinin affect receptor binding and immune response. Proc Natl Acad Sci USA 2009; 106: 18137-42.

[25] Karaivanova VK, Spiro RG. Sulphation of N-linked oligosaccharides of vesicular stomatitis and influenza virus envelope glycoproteins: host cell specificity, subcellular localization and identification of substituted saccharides. Biochem J 1998; 329: 511-8.

Received: May 31, 2011 Revised: March 19, 2012 Accepted: March 28, 2012